Supplementary information

Insights into the phenomenon of '*bubble-free*' electrocatalytic oxygen evolution from water

George Tsekouras,*[a,b] Richard Terrett,[c] Zheyin Yu,[d] Zhenxiang Cheng,[d] Gerhard F. Swiegers,*[b] Takuya Tsuzuki,[a] Robert Stranger,[c] Ronald J. Pace*[c]

[a] *Research School of Electrical, Energy and Materials Engineering, The Australian National University, Acton, ACT 2601, Australia. E-mail: george.tsekouras@anu.edu.au*

[b] *Intelligent Polymer Research Institute and Australian Research Council Centre of Excellence for Electromaterials Science, University of Wollongong, Wollongong, NSW 2522, Australia. E-mail: swiegers@uow.edu.au*

[c] *Research School of Chemistry, The Australian National University, Acton, ACT 2601, Australia. E-mail: ron.pace@anu.edu.au*

[d] *Institute for Superconducting and Electronic Materials, Australian Institute of Innovative Materials, University of Wollongong, Wollongong, NSW 2522, Australia.*

Experimental

Catalyst-binder layer preparation

Raney Ni is prepared by leaching a Ni-Al alloy, typically containing small amounts of other metals, in concentrated NaOH, in order to selectively remove the aluminium and leave behind a porous, high surface area catalyst. Raney Ni promoted with 2% Fe and 2.5% Cr (Alfa Aesar, A-4000) was selected here for its iron content, where the combination of Ni and Fe is known to be very active for the oxygen evolution reaction (OER).[1-4]

Raney Ni was milled prior to use until the particle size was smaller than the apertures of the Ni mesh current collector (Century Woven, 200 LPI, ø 50 μm wire, 75 μm aperture, Fig. S1). Decanted Raney Ni aqueous slurry with 10 g equivalent dry weight was combined with 100 g of ø 6 mm steel balls and 18 mL deionised water in a gasket-sealed steel cup and milled for 1 h in a SPEX 8000M Mixer/Mill®. Opening of the steel cup and associated breaking of the gasket seal after milling was accompanied by a momentary audible fizzing sound. This was ascribed to hydrogen gas, originally produced during NaOH leaching of Ni-Al alloy, having been released from the pores of the Raney Ni during the vigorous, high-energy milling process.

The milled Raney Ni aqueous slurry was dried overnight at room temperature to a powder, in order to simplify and improve the accuracy of ink formulation. No sign of spontaneous combustion was observed the following day, suggesting that milling had eliminated the pyrophoric character of the as-received Raney Ni. This might be explained by the apparent removal of hydrogen gas from Raney Ni pores during milling as described above, thus removing the fuel required for a pyrophoric event.

Fig. S2 shows an overlay of steady-state current-voltage curves comparing the OER activity of breathable electrodes based on as-received, or milled and dried, Raney Ni, where each curve is the average of triplicate samples. According to the very similar responses observed, it may be concluded that milling and drying of Raney Ni had no adverse effect on OER activity.

Catalyst-binder inks, each with a total solvent volume of ~5 mL, were prepared by combining Raney Ni, poly(tetrafluoroethylene) (PTFE) powder (Alfa Aesar, A12613, 15–25 µm particle size), carbon black (CB) powder (Alfa Aesar, 39724, 42 nm average particle size), isopropyl alcohol (IPA), and deionised water. Note that CB was included in catalyst inks as a conductive thickener. Mixing was carried out for 2 min in the mixer/mill using a ø 3 mm steel ball.

Catalyst-binder layer preparation proceeded as follows. The Ni mesh current collector, laser-cut to yield a 1 cm^2 disk active area, and cleaned by ultrasonication in IPA, was dip-coated in the catalyst-binder ink and hung vertically to semi-dry for ~10 min at room temperature, before a second and final dip-coat was performed, followed by complete drying at room temperature. The sample was then passed through a roller in order to flatten the coating out evenly over the current collector. This was followed by heat treatment in a tube furnace under flowing nitrogen for 2 h at 350 °C, which is 20–30 °C above the vendor-specified melting point of PTFE (320–330 °C), in order to bind the electrode. The nitrogen exiting the tube furnace, which might have contained toxic fluorinated species derived from the PTFE, was safely vented. A short length of PTFE thread seal tape was then wrapped around the part of the Ni mesh current collector adjacent to the 1 cm^2 disk active area, and compressed at 40 MPa using a hydraulic press, in order to mask it and prevent it from participating in the OER. The final electrode had a typical Raney Ni catalyst loading of ~35 mg cm^{-2}.

Fig. S3 shows scanning electron micrographs of the surface of a catalyst-binder layer comprising 56 wt.% Raney Ni, 40 wt.% PTFE, and 4 wt.% CB (=29 vol.% Raney Ni, 63 vol.% PTFE, and 8 vol.%

CB). The images are complementary and were recorded using backscattered electron (BE) and secondary electron (SE) detectors. The BE image shows bright Raney Ni particles ranging in size between ~1–10 μm in a dull matrix composed largely of PTFE. The SE image shows wavy patterns that may be attributed to melted PTFE, and bright particles that may be attributed to CB based on their size.

Breathable electrode preparation

The gas-generating catalyst-binder layer on its own was incapable of bubble-free operation, and was integrated with gas-extracting expanded PTFE (ePTFE) membrane (Gore-Tex®) in order to afford a breathable electrode. The starting point of breathable electrode preparation was a poly(propylene) (PP) block with dimensions 50 mm (height) × 25 mm (width) × 10 mm (thickness) (Cammthane). A ø 1.5 mm hole was drilled into the front face of the PP block, and a ø 4.2 mm hole was drilled into the top edge of the PP block. The ø 4.2 mm hole was then tapped to allow for the fitting of a threaded-to-tube adaptor (SMC, KQ2H06-M5N). The ø 1.5 mm and ø 4.2 mm holes met at right angles within the PP block to allow for the application of vacuum behind the ePTFE membrane. A 15 mm × 15 mm piece of PP spacer (ø 250 μm thread, 1250 μm aperture, Fig. S4) was then thermally tacked over the ø 1.5 mm hole, to ensure even vacuum across the back of the ePTFE membrane. A 20 mm × 20 mm piece of ePTFE membrane supported by non-woven PP backer (General Electric, Preveil, 0.2 μm pore size) was then thermally welded to the PP block. Prior to carrying out the next step, the PP block/PP spacer/ePTFE membrane assembly was placed in deionised water and a vacuum of 50 kPa applied behind the ePTFE membrane for 2 min to check for leaks. After the leak check was passed, 45 wt.% PTFE (Alfa Aesar, A12613, 15–25 μm particle size) in IPA was mixed in the mixer/mill for 2 min using a ø 3 mm steel ball, before 150 μL of the resulting dispersion was drop-cast onto the ePTFE membrane to afford the PTFE interlayer. Without delay, the previously prepared catalyst-binder layer was wet-laminated onto the PTFE interlayer and thermally tacked onto the PP block.

Electrochemical cell

The 3-electrode electrochemical cell was comprised of a breathable working electrode, a Ni mesh counter electrode, and a Hg/HgO reference electrode (Bioanalytical Systems, Inc., RE-61AP) filled with 1M KOH aqueous electrolyte. The vessel was constructed of transparent acrylic, employed threaded-to-tube adaptors for electrolyte inlet and outlet (John Guest, PM010602E), and included a lid with holes to accommodate working electrode, counter electrode, reference electrode, nitrogen purge line, and thermometer. Nitrogen was constantly bubbled through the 1M KOH aqueous electrolyte in order to prevent dissolution of $CO_{2(g)}$ from the air and subsequent reaction with $KOH_{(aq)}$ to form insoluble $K_2CO_{3(s)}$.

Due to the temperature-dependence of Hg/HgO reference electrode voltage,[5] only the very tip of the reference electrode was dipped in the electrolyte during measurements above room temperature, with most of the reference electrode body sitting above the vessel lid. This approach was confirmed to be effective by checking the voltage of the reference electrode before, and immediately following, a 2 h, 60 °C test, against a second Hg/HgO reference electrode that had been kept at room temperature for the duration of the test. The voltage of the reference electrode was within 2 mV of the second reference electrode both before and immediately following the test.

Testing system

ΔP was generated by applying a vacuum behind the ePTFE membrane, with the electrolyte kept at ambient pressure. This approach was deemed easier compared to designing and building a pressurised vessel, in which case ΔP would have been generated by pressurising the electrolyte with a static head of inert gas, while the space behind the ePTFE membrane would have been kept at ambient pressure. However, the use of a vacuum here resulted in trade-offs, namely the possibility of the electrolyte

boiling at temperatures below 100 °C (*e.g.* water boils at 60 °C under –80 kPa vacuum, to give an indication),[6] and mixing of product oxygen with compressed air, which precluded its analysis.

The testing system with ΔP and temperature control worked according to the following. Compressed air was continuously passed through the Venturi vacuum generator (SMC, ZH05BS-06-06, –88 kPa). ΔP across the ePTFE membrane was controlled by adjusting the needle valve (Process Systems, NVS-02), and monitored using the vacuum gauge (WIKA, 7203736). Electrolyte was circulated through the electrochemical cell and heat exchanger (Alfa Laval, Alfa Nova 14-4H) using a pump (Flojet, D3131-E5011, 12 V DC), a power supply (Techbrands, MP3241, 10 A, 12 V DC), and a speed controller (Techbrands, MP3209, 8 A, 12 V DC). The heater/pump (PolyScience® temperature controller) was connected to the heat exchanger, and the temperature set point adjusted until the desired temperature reading was observed on the thermometer submerged in the electrolyte within the electrochemical cell. Compressed air, vacuum, electrolyte, and heated water lines were all made of chemically-resistant perfluoroalkoxy alkane (PFA) tubing (Swagelok, PFA-T6M-1M-30M). The testing system had ΔP and temperature specifications of 0–80 kPa and 20–60 °C, respectively.

Electrochemical measurements

All electrochemical measurements were performed using a BioLogic VSP potentiostat/galvanostat. Steady-state current-voltage measurements were carried out by stepping the current density between 5, 10, 15, 20, 25, 30, 40, 50, 75, and 100 mA cm^{-2}, holding each step for 20 s, and measuring the voltage at an acquisition rate of 5 Hz. To avoid capturing the capacitive response, only the voltage measured between t = 10–20 s for each step was averaged and reported. Voltages were converted from relative to the Hg/HgO reference electrode to relative to the reversible hydrogen electrode (RHE) according to the equation $E_{RHE} = E_{Hg/HgO} + 0.098 + (0.0592 \times pH)$.

All electrochemical data was corrected for current × resistance (iR) drop. R was determined using galvanostatic electrochemical impedance spectroscopy (GEIS) under 10 mA cm^{-2} DC bias, with 10 mA cm^{-2} AC perturbation, and between 50 kHz and 10 Hz. Fig. S5 shows an example Nyquist plot for a breathable electrode and the result of fitting using the equivalent circuit shown. The series resistance element "R1" extracted from the fit was used to perform iR correction.

Double-layer capacitance (C_{DL}) measurements were carried out to gauge the electrochemical surface area of breathable electrodes at open-circuit under different ΔP and temperature conditions. The voltage was swept between +50 mV and –50 mV about the open-circuit-voltage at scan rates of 100, 50, 20, 10, and 5 mV s^{-1}, and with a 10 s holding period at each of the voltage limits.[7] Fig. S6 shows an example C_{DL} measurement for a breathable electrode. For each scan rate, positive and negative capacitive current values at a fixed voltage were noted, the latter subtracted from the former, and the result divided by two to yield the capacitive current (i_C). This was plotted against scan rate (v) and a linear function fitted to the data, the slope of which was equal to C_{DL} according to the equation $i_C = C_{DL} v$.

Extended discussion

Temperature-dependence of breathability problem

Equation (3) explains the temperature-dependence of the breathability problem. Following the same procedure as described in the main article, a γ value of 0.06651 N m^{-1} is calculated for 1M KOH at 60 °C. Substituting this value into Equation (3), and reasonably assuming that θ decreases with increasing temperature, a P_C value less negative than –45 kPa would be calculated, which would make the PTFE interlayer more susceptible to flooding at 60 °C compared to 20 °C. This is consistent with Fig. 9c, where the onset of impaired breathability, indicated by the inflection point between trough and lead-out responses, shifted from 45 kPa at 20 °C, to 25 kPa at 60 °C.

Making the poly(tetrafluoroethylene) interlayer more resistant to flooding

The PTFE interlayer may be made more resistant to flooding with electrolyte by making its P_C value more negative. According to Equation (3), this can be realised by lowering the denominator, r, which in turn may be achieved by employing a PTFE powder with a smaller particle size than that used in this study (15–25 µm). For example, spherical 5 µm particles in hexagonal close packed arrangement yield an r value of 0.6 µm, which when substituted into Equation (3) together with γ and θ values of 0.07264 N m^{-1} and 133°, respectively, yields a P_C value of –165 kPa ($T = 20$ °C). This is significantly more negative than the P_C value of –45 kPa calculated in the main article when 20 µm particles were assumed. The use of finer PTFE powder for the PTFE interlayer should therefore permit the application of significantly higher ΔP without the risk of flooding the PTFE interlayer. In turn, this should permit enhanced performance due to increased electrochemical surface area.

Enhanced performance expected by raising flooding resistance of poly(tetrafluoroethylene) interlayer

For example, we begin by noting that, according to Fig. 9c, the maximum ΔP that can be applied at 60 °C before breathability begins to be impaired is 25 kPa. Under these conditions, Fig. 8c indicates a normalised C_{DL} value of ~0.6, which means that only ~60% of the catalyst-binder layer participates in the OER. Fig. 8c also shows that raising ΔP from 25 kPa to 60 kPa would result in near-complete wetting of the catalyst-binder layer, a ~40% increase in available electrochemical surface area, and therefore the likelihood of significantly enhanced performance.

Pore radius calculation

To calculate pore radius, PTFE particles were assumed to be spherical and to be in hexagonal close packed arrangement. The starting point is a top-view schematic of four spherical PTFE particles (in blue) in hexagonal close packed arrangement (Fig. S9a). Removal of the top PTFE particle reveals a spherical pore (in green) (Fig. S9b). Fig. S9c shows the subsequent removal of the upper PTFE particle and forward-tilt such that the isosceles triangle connecting the centres of the remaining PTFE particles and of the pore are in the plane of the page. Recognising that the centres of the PTFE particles in Fig. S9a form a regular tetrahedron, the isosceles triangle exhibits a vertex angle of 109°28'16" (~109.47°),[8] a base measuring $2r_{PTFE}$, and legs each measuring $r_{PTFE} + r_{pore}$ (Fig. S9d). Cutting the isosceles triangle along its axis of symmetry gives a right-angled triangle with angle ~54.74°, opposite side measuring r_{PTFE}, and hypotenuse measuring $r_{PTFE} + r_{pore}$ (Fig. S9e). The following trigonometric relationship applies to the right-angled triangle in Fig. S9e:

$$\sin 54.74° = \frac{r_{PTFE}}{r_{PTFE} + r_{pore}}$$

Assuming an r_{PTFE} value of 10 µm (d_{PTFE} = 20 µm) yields an r_{pore} value of 2.2 µm.
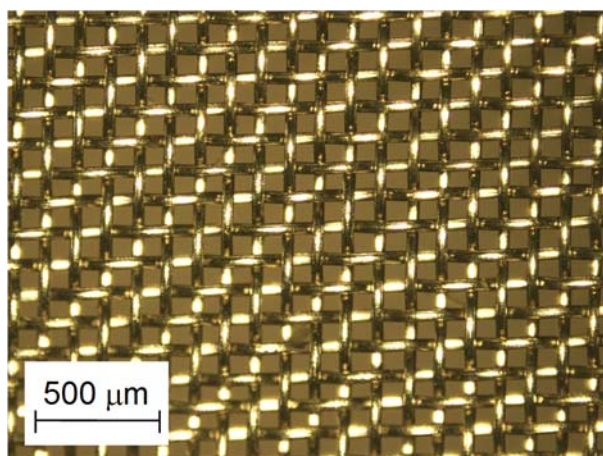
Fig. S1 Optical microscope image of Ni mesh current collector. Century Woven, ø 50 µm wire, 75 µm aperture.
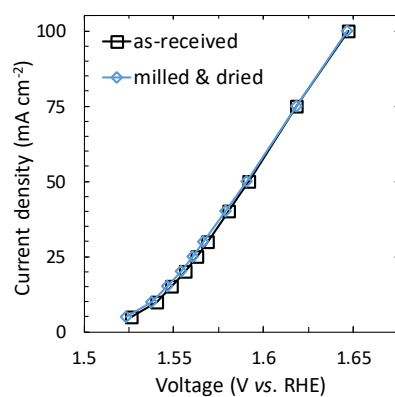
Fig. S2 Steady-state current-voltage curves of breathable electrodes based on as-received, or milled and dried, Raney Ni catalyst. 1M KOH, 20 °C, 50 kPa ΔP.
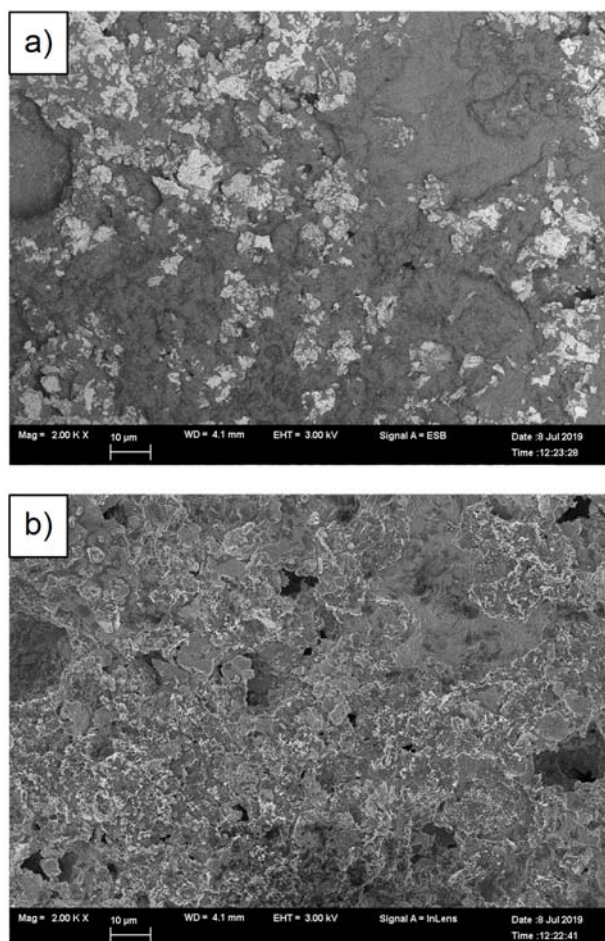
Fig. S3 Scanning electron micrographs of a fixed area of a catalyst-binder layer sample composed of Raney Ni, PTFE, and carbon black. a) Backscattered electron image. b) Secondary electron image.
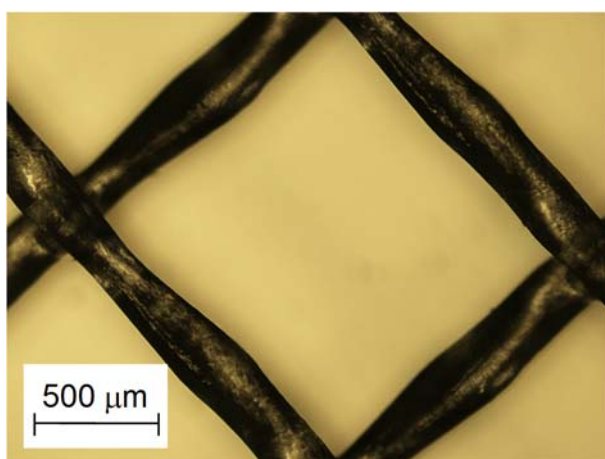
Fig. S4 Optical microscope image of poly(propylene) spacer. ø 250 μm thread, 1250 μm aperture.
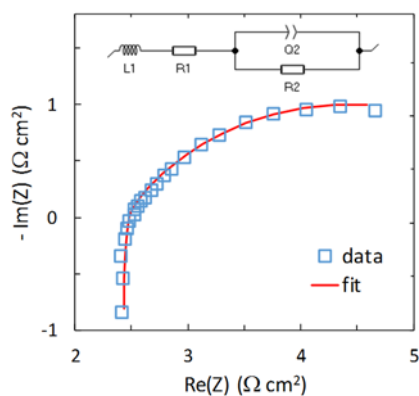
Fig. S5 Nyquist plot of a breathable electrode. 10 mA cm^{-2} DC bias, 10 mA cm^{-2} AC perturbation, 50 kHz → 10 Hz. Inset: equivalent circuit used to fit data. 1M KOH, 20 °C, 50 kPa ΔP.
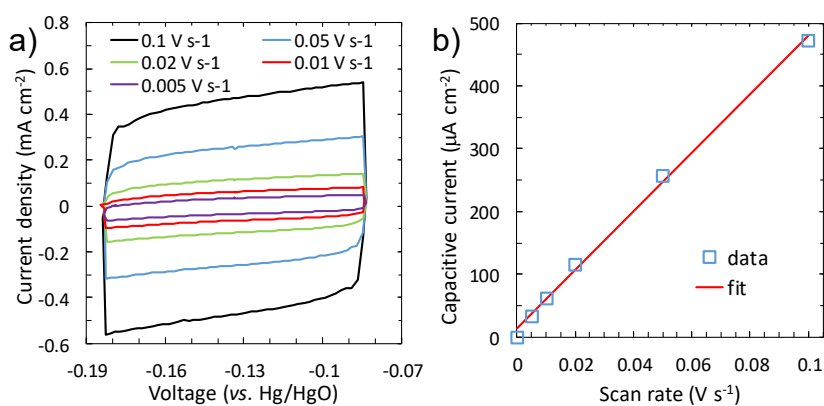
Fig. S6 Double-layer capacitance of a breathable electrode. a) Cyclic voltammograms. b) Capacitive current *vs*. scan rate. 1M KOH, 20 °C, 80 kPa ΔP.
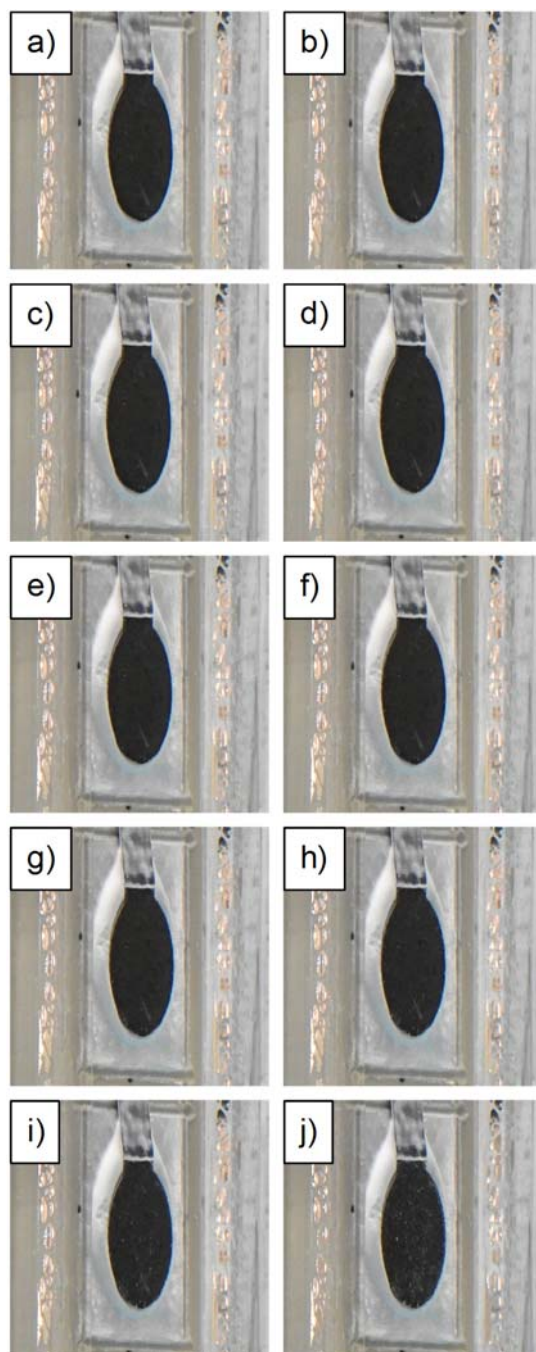
Fig. S7 Appearance of a breathable electrode at different current densities: a) 5 mA cm⁻², b) 10 mA cm⁻², c) 15 mA cm⁻², d) 20 mA cm⁻², e) 25 mA cm⁻², f) 30 mA cm⁻², g) 40 mA cm⁻², h) 50 mA cm⁻², i) 75 mA cm⁻², j) 100 mA cm⁻². 1м KOH, 20 °C, 50 kPa ΔP.
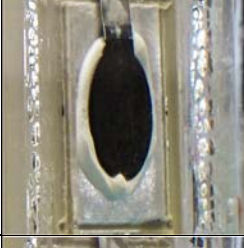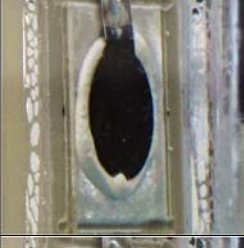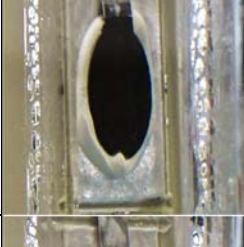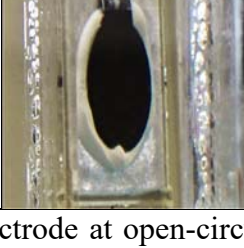
ΔP (kPa) \ T (°C)	20	60
0		
10		
20		
30		
40		
50		
60		

Fig. S8 Appearance of a breathable electrode at open-circuit for combinations of temperature and pressure differential. 1M KOH.
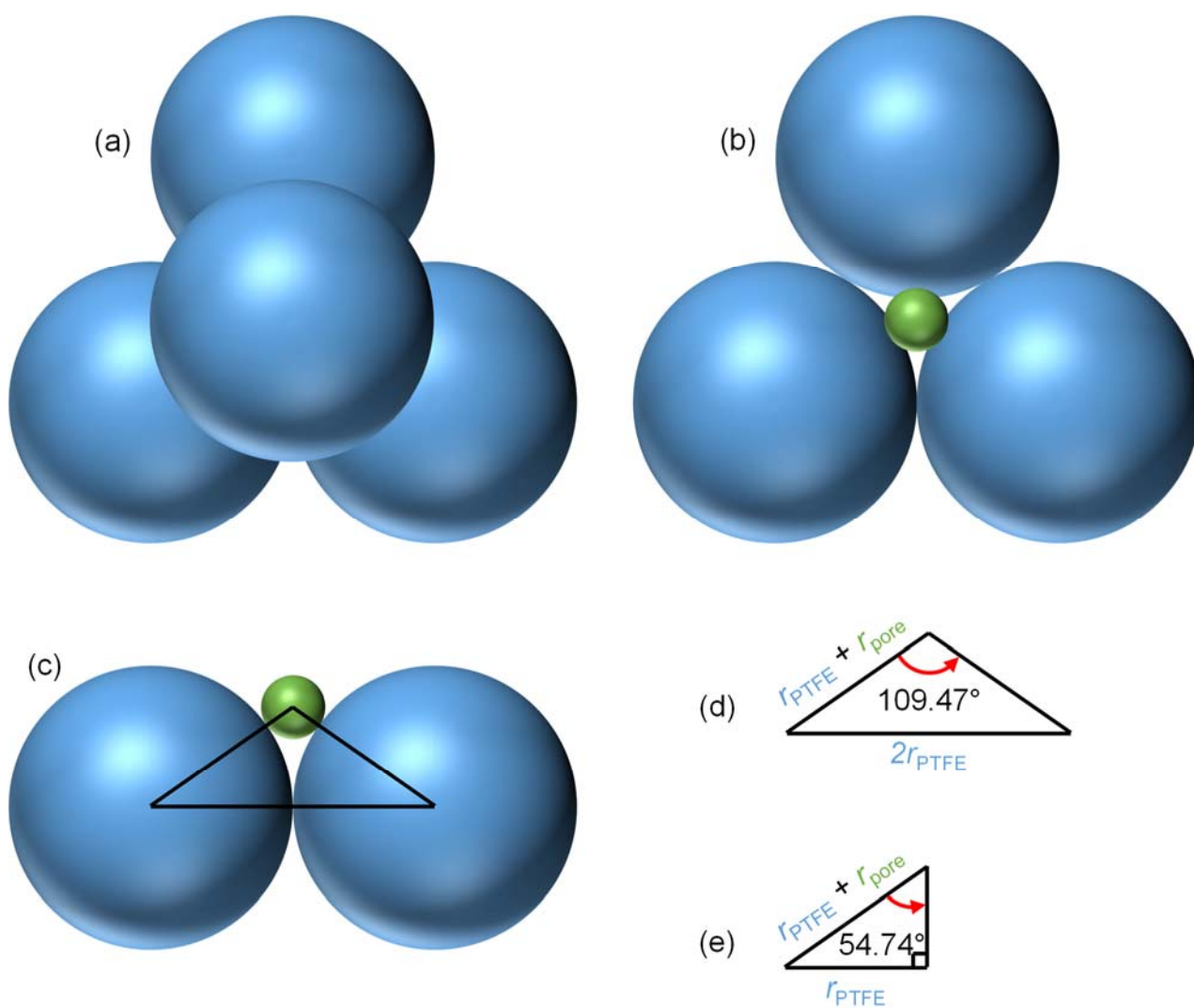
Fig. S9 (a) Top-view schematic of four spherical PTFE particles (in blue) in hexagonal close packed arrangement. (b) Removal of top PTFE particle revealing a spherical pore (in green). (c) Removal of upper PTFE particle and forward-tilt such that isosceles triangle connecting centres of remaining PTFE particles and of pore are in the plane of the page. (d) geometry of isosceles triangle. (e) geometry of right-angled triangle obtained by cutting isosceles triangle along its axis of symmetry.

References

1. D. A. Corrigan, *J. Electrochem. Soc.*, 1987, **134**, 377-384.

2. M. W. Louie and A. T. Bell, *J. Am. Chem. Soc.*, 2013, **135**, 12329-12337.

3. L. Trotochaud, S. L. Young, J. K. Ranney and S. W. Boettcher, *J. Am. Chem. Soc.*, 2014, **136**, 6744-6753.

4. J. R. Swierk, S. Klaus, L. Trotochaud, A. T. Bell and T. D. Tilley, *J. Phys. Chem. C*, 2015, **119**, 19022-19029.

5. S. Rondinini, P. Longhi, P. R. Mussini and T. Mussini, *Pure & Appl. Chem.*, 1994, **66**, 641-647.

6. Water-Saturation Pressure, https://www.engineeringtoolbox.com/water-vapor-saturation-pressure-d_599.html, (accessed October 2020).

7. C. C. L. McCrory, S. Jung, J. C. Peters and T. F. Jaramillo, *J. Am. Chem. Soc.*, 2013, **135**, 16977-16987.

8. W. E. Brittin, *J. Chem. Educ.*, 1945, **22**, 145.